Ultraviolet photoemission studies of the oxidation of thin Bi films using synchrotron radiation*†

R. L. Benbow and Z. Hurych
Physics Department, Northern Illinois University, DeKalb, Illinois 60115
(Received 8 April 1976)

Three aspects of photoelectron spectroscopy are used to examine the oxidation process in thin Bi films with cleaved layered crystals of V*B*-VI*B* compounds used as substrates. Valence-band emission, 5*d* core emissions, and the conduction-band density of states are all examined separately. The changes in the electronic structure shows that oxidation occurs in three stages as oxygen exposure increases: (i) a precursor stage of weak chemisorption; (ii) a sudden onset of strong rapid oxidation and growth of a two-dimensional oxides; and (iii) a slower growth of the oxide layer. Bi 5*d* core-level shifts, the opening of a band gap at the Fermi level, and spin-orbit splitting in the conduction band in the oxide are all discussed.

I. INTRODUCTION

The oxidation of metals is a well-known and much-studied subject. It is known generally that the process is dependent upon a number of things—surface smoothness, temperature, partial pressure of oxygen, and in the case of single crystals, the type of crystal face involved. The steps involved in the oxidation process are not well known, but, in general, seem to be a function of the metal involved. For example, Cs apparently begins to oxidize by dissolving oxygen ions below the metal surface, and then having a series of different oxides materialize as the oxygen exposure increases.[1] The oxidation of Sr appears to begin in the same manner, but only one oxide appears.[2] Neither of these forms a protective layer and so oxidation continues as long as exposure continues. Nb, on the other hand, seems to begin by dissolution of oxygen ions and also forms a complicated series of oxides, but does eventually passivate.[3] Other metals, such as Al, very quickly form a tough protective oxide that prevents further rapid oxidation of the metal. Still others, such as Pt and Ir are somewhat unaffected by the presence of O, although some chemisorption may take place under special conditions.[4,5]

Bi, on the other hand, seems to be quite inert, although not to the extent of the noble metals. The basic inertness of Bi is tied to the concept of a semimetal. Let *et al.*[6] used x-ray-photoemission-spectroscopy studies of As, Sb, and Bi in crystalline and amorphous states to show that covalent bonding may play a significant role in the three semimetals. In general, the valence structure of Bi was found to consist of a low-lying set of 6*s* bands and a spin-orbit split doublet of 6*p* bands just below the Fermi level, in agreement with band-structure calculations.[7] The total width of the 6*p* bands was 5.2 eV, somewhat larger than estimated by the band-structure calculations.[7] The doublet structure persisted in the amorphous as well as the crystalline state.

The present work was done on evaporated films of varying quality and manufacture instead of idealized, cleaned single-crystal faces. The continuum nature of synchrotron radiation was used to provide three interrelated mechanisms to study the oxidation of the Bi films: (i) conventional energy-distribution curves (EDC's) were made to monitor changes in the valence-band density of states (VBDOS) as a function of oxygen exposure; (ii) Bi 5*d* core states were observed and their energy levels were found to shift upon oxidation; and (iii) the constant final-energy spectroscopy[8] (CFS) was used to observe changes in the (empty) conduction-band density of states (CBDOS). The photoionization cross section for 6*s* electrons is much smaller than that for 6*p* electrons in the vacuum ultraviolet region of the spectrum, and so only the latter were observed in the VBDOS.

In Sec. II we consider the experimental aspects. In Sec. III we present results which are then discussed in Sec. IV.

II. EXPERIMENTAL PROCEDURES

The entire project was carried out at the University of Wisconsin Synchrotron Radiation Center. Tunability of the synchrotron continuum is achieved through use of a McPherson 225 normal incidence monochromator. Monochromatized light emerging from the exit slit diverges rapidly and is focused onto the sample by a grazing incidence elliptical mirror. The optical system and experimental chamber are described in more detail elsewhere.[9]

The sample chamber has a base pressure of $5 \times (10)^{-10}$ Torr. The samples were prepared *in situ* by first cleaving a layered Bi_2Te_3 or Sb_2Te_3 crystal and then evaporating Bi onto it to the desired thickness. The cleavage plane of these layered crystals (of the V*B*-VI*B* class) are atomically smooth and

inert and form idealized substrates.[10] The thickness of the films was estimated from the change in frequency of a quartz-crystal thickness monitor. The Bi was evaporated slowly (4–10 Å/min) to maintain a pressure $\lesssim 10^{-8}$ Torr during evaporation.[11]

After evaporation, the sample was positioned at the object point of the Physical Electronics double-pass cylindrical-mirror analyzer (CMA) and monochromatic radiation was shined onto it. EDC's were obtained at photon energies of 10.2, 14.5, and 18.0 eV. These photon energies allow convenient examination of the valence-band region of the density of states. Also, the lower energy part of an EDC was obtained at 38.0 eV, from which the position of the low-lying 5*d* core states of Bi could be observed.

Next, the constant final-energy spectra (CFS's) were made.[8] This was accomplished by fixing the acceptance energy (i.e., by using a constant retarding voltage) of the CMA and using the wavelength drive on the monochromator to sweep through a range of photon energies. The CFS's are sensitive to the Auger decay of excited core holes—even when the excited core electron cannot be photoemitted. (It is also possible to detect direct emissions from the core states in a CFS.) CFS's were made at two or three kinetic energies.

After a set of EDC's and CFS's were acquired, the sample would be exposed to O_2 at a constant pressure for a fixed time. Then the same set of EDC's and CFS's would be obtained again. This process was repeated so as to increase the total exposure in langmuirs (1 L = 10^{-6} Torr sec) incrementally on a logarithmic scale. It is significant to note that because of the very large range of exposures (from 0 up to 10^7 L), the incremental exposures were not all made at the same pressure as would be desired. For small exposures, low pressures (~10^{-8}–10^{-7} Torr) were used for times of the order of 10^2–10^3 sec. For the largest exposures, pressures of the order of 10^{-4}–10^{-3} Torr would be used for 10^3–10^4 sec. After such high-pressure exposures, the pressure in the chamber would remain one or two orders of magnitude higher than the base pressure. If a small exposure were to be made at a high pressure for even a short time, the residual O_2 in the system would continue to make a *relatively* large exposure even after pumpdown. It is also significant to note that the pressure for a succeeding exposure was maintained at the same value whenever a set of curves showed noticeable differences from a preceding set. For example, for the film shown below, the exposures of 10^5, 2×10^5-, and 4×10^5-L O_2 were all made at a pressure of 10^{-4} Torr.

The useful data that come out of this lengthy process are the changes recorded in the EDC's and CFS's as a function of the total exposure.

III. EXPERIMENTAL RESULTS

EDC's for Bi at various exposures to O_2 are shown in Figs. 1–3. In Fig. 1 we see EDC's at a photon energy $h\nu = 10.2$ eV for Bi. These are characterized by a sharp peak at −3.1 eV and a broader less-prominent peak at −1.4 eV. There is a third structure appearing as a shoulder at −4.3 eV. The EDC's for Bi at $h\nu = 14.5$ eV (Fig. 2) are considerably different. There is the large inelastic peak at low energy and peaks at −1.3 and −3.7 eV labeled *A* and *B*, respectively. These same features are also present in the EDC's at $h\nu = 18.0$ eV (Fig. 3), but at −1.4 and −3.6 eV. Peaks *A* and *B* in the EDC's at 14.5 and 18.0 eV are the spin-orbit-split 6*p* bands observed in x-ray photoemission spectroscopy data[6] and predicted by band structure.[7] The structures are different at $h\nu = 10.2$ eV because the effect of the joint density of states predominates. The EDC's at 10.2 eV for our films show many features of, but less detail than, EDC's at 10.2 eV of Lapeyre *et al.*[12] on single crystals of Bi.

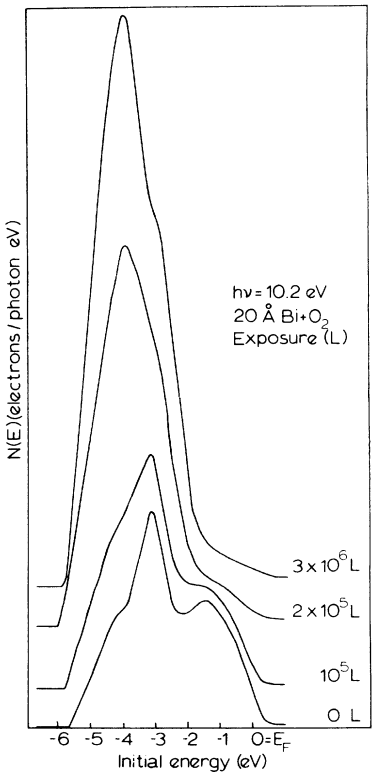

FIG. 1. Normalized EDC's at $h\nu = 10.2$ eV. Included are those for unexposed Bi, two intermediate O_2 exposures, and the most heavily exposed situation.

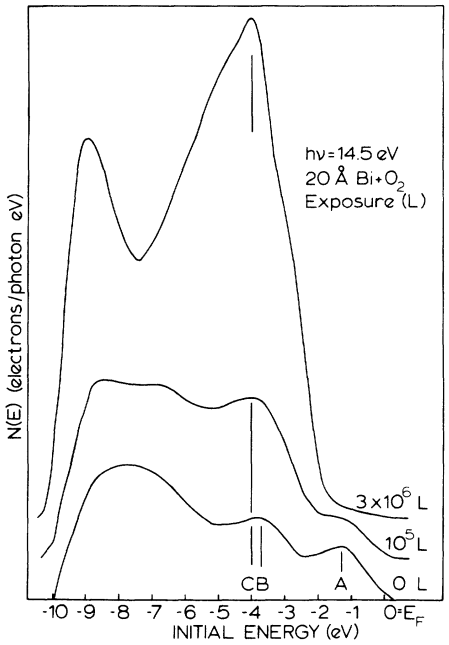

FIG. 2. Normalized EDC's at $h\nu = 14.5$ eV. Included are one for unexposed Bi, another for an intermediate exposure, and a third for the maximum exposure.

There are (some) features common to the EDC's at all three photon energies when the sample was exposed to oxygen. (a) The shape of EDC's showed only weak changes below exposures of 10^4–10^5 L of O_2. (b) Then in a relatively narrow range (on a logarithmic scale) of exposure the shape of the EDC's changed rather dramatically. Further, the overall width would decrease by about 1.9 eV, except for a greatly attenuated "tail" just below the Fermi energy. (c) The photoyield would increase by an order of magnitude.[13]

Attenuation of features just below the Fermi level and changes in the photoyield are evident in the EDC's shown in Figs. 1–3. In addition, the peak labeled B in Figs. 2 and 3 gives way to a much more powerful one labeled C. It is unfortunate that the energy of the oxygen p levels (nominally peak C in Figs. 2 and 3) coincides with the lower energy peak in the Bi density of states (peak B). Further, another weak peak labeled D appeared at $E = -7$ eV for $h\nu = 18.0$ eV. The actual changes recorded in the EDC's varied from film to film, but these basic features persisted in some form for every film tested.

The low-energy portion of the EDC's at 38.0 eV provided a different viewpoint. In Fig. 4 we see the direct emissions from the $5d_{5/2}$ and $5d_{3/2}$ core states in Bi at -23.8 ± 0.1 eV and -26.9 ± 0.1 eV, respectively, in close agreement with the x-ray photoemission data.[6] These are less sensitive to the presence of oxygen than the valence-band emissions, although the ultimate changes are just as significant. The binding energy of the core levels increases by 1.9 eV upon oxidation. Also in Fig. 4 we observe that the change is not abrupt;

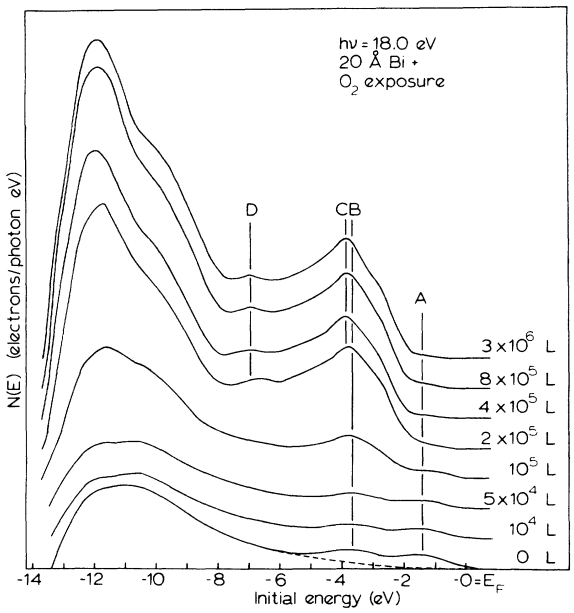

FIG. 3. Normalized EDC's at $h\nu = 18.0$ eV. These cover the wide range of exposures from 0 L of O_2 to 3×10^6 L of O_2.

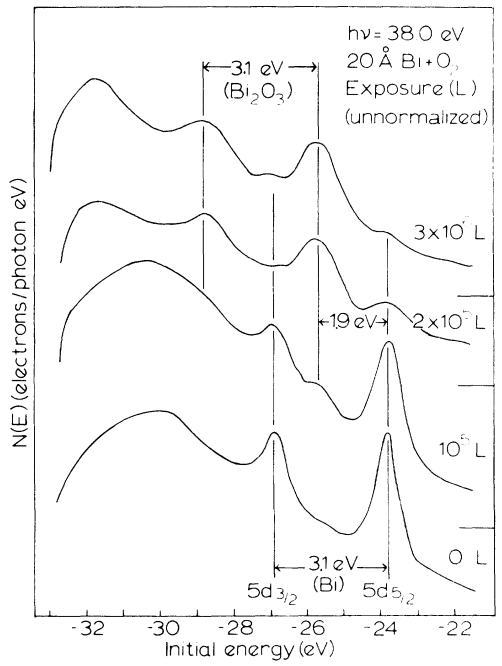

FIG. 4. Incomplete EDC's at $h\nu = 38.0$ eV. These are un-normalized but do show the effect of various exposures to O_2 on the Bi $5d$ core emissions.

it occurs in a range of exposures. One set of peaks (Bi) is attenuated while the second set of peaks (Bi $+O_2$) rise out of the background. Note that at an intermediate exposure, parts of both sets of peaks are clearly present. The fact that the Bi structure is attenuated corresponds to the oxide forming on the surface.[14] (There is no problem in identifying the correct peaks: they are spin-orbit split by 3.1 eV and the $5d_{5/2}$ emission is much stronger than the $5d_{3/2}$ emission.)

The CFS's are also quite interesting and more useful than the EDC's at $h\nu = 38.0$ eV. For unexposed Bi, the CFS shows the structure resulting from the Auger decay of the $5d$ core holes in Bi. (The CFS would also show the direct emissions from these core electrons, but they occur at higher photon energies—how high being a function of the acceptance energy of the CMA. No effort has been made to include these direct emissions in the presentation of the data; they were omitted for the sake of clarity.) The changes in these structures occur at the same time that changes occur in the valence-band emissions, and are subtle at first and quite pronounced when the process is completed. Figure 5 shows the changes for the same sample as in Figs. 1–4. The large Bi $5d_{5/2}$ Auger peak (labeled U) is attenuated rapidly upon the onset of oxidation and all but disappears. The same may be said of the $5d_{3/2}$ peak (labeled V). (Not shown, but observed, was the fact that direct emissions from the $5d$ core states shifted to photon energies which were higher by 1.9 eV.) New Auger structures appear in the oxidized film. Specifically, in the Bi film peaks U and V were observed at $h\nu = 24.5$ and 27.6 eV, with the low-energy onsets at $h\nu = 23.8$ and 26.9 eV, respectively. In the O_2-exposed Bi film, peaks X, Y, and Z appear at $h\nu = 26.2$, 27.3, and 29.25, and a shoulder appears at 30.4 eV (all energies are ±0.1 eV). Note that peak Z is the most prominent.

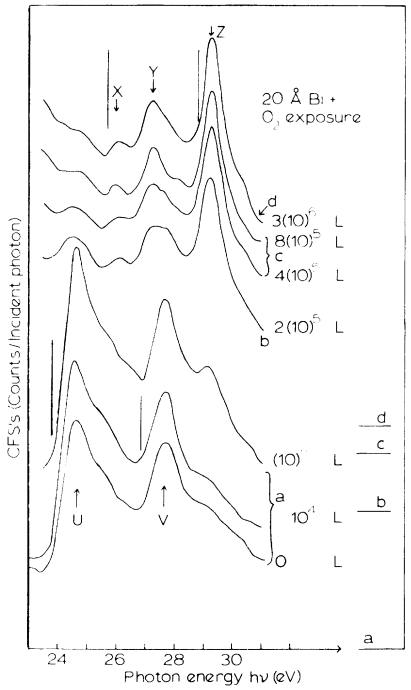

FIG. 5. CFS's between $h\nu = 23$ and 31 eV. These are normalized and corrected for the varying light flux out of the monochromator. The core level indications reflect the instrumental resolution at these photon energies as opposed to the visible onset of the peaks.

To summarize the results we may say that the oxidation of Bi takes place in three stages. The first stage is characterized by an overall decrease in photoyield and by very minor changes in the valence band emissions and corresponds to a weak chemisorption of oxygen. The conduction bands are not affected nor are the $5d$ core levels. There is a slight charge redistribution affecting the valence electrons with energies nearest the Fermi level.

The second stage is characterized by the sudden and rapid changes in all structures: the EDC's are altered in shape and magnitude; a band gap opens up; the Bi $5d$ core emissions shift downward 1.9 eV from their original position; and the conduction-band density of states (characterized by the CFS's) rapidly distorts to a form bearing little resemblance to the original structure.

The final stage is characterized by relative stability in the appropriate features of the three types of spectra considered here, although it must be pointed out that similar conclusions could be drawn if it happened that the oxide thickness exceeded the electron escape depth. (Recall, however, that there is a remnant of metallic emission near the Fermi level, which could be attributed to the unoxidized metal, or even the substrate, beneath the oxide layer.)

IV. DISCUSSION

The interpretation of the results begins with the fact that for many metals, e.g., the transition metals, exposures of only a few L of O_2 (usually much less than 10^2) to clean surfaces results in strong chemisorption of oxygen and oxide formation. In the case of Bi, there is apparently a precursor stage of adsorption of oxygen below a critical exposure (and/or pressure). This precursor state is discernible by the slight decrease in photoyield and the slight change in shape of the VBDOS at the lower exposures. Beyond this initial state, strong chemisorption or actual oxidation begins. This accelerating adsorption or oxidation is ex-

emplified by the steplike behavior of the curves in Fig. 6, in which basic features of the EDC's at $h\nu = 18.0$ eV are plotted as a function of total exposure. Such behavior is typical of a nucleation process, which, once begun, accelerates toward its final state. Such a process is fairly well documented in the case of Fe.[15] According to the low-energy-electron-diffraction and Auger-electron-spectroscopy study by Simmons and Dwyer,[15] Fe initially adsorbs O_2 which in turn is dissociated and chemisorbed. When the chemisorptive state is saturated, FeO nucleates and the sticking coefficient of oxygen increases during formation of a two-dimensional oxide layer. The sticking coefficient subsequently decreases as three-dimensional oxide growth begins. In the present case, we have not the capabilities for detailed surface analysis required to state the actual condition of the surface of the films. Rather, we draw our inferences from the electronic details of the few layers nearest the surface.

The height of the peak at the Fermi level is relatively slowly attentuated up to an exposure of 5×10^4 L of O_2, at which point it is attenuated more quickly and ultimately disappears, becoming instead, a weak "tail." This attenuation is exhibited by curve (d) in Fig. 6. {The points corresponding to the areas in Fig. 6 at an O_2 exposure of 4×10^5—i.e., in curves (a) and (b)—appear to be anomalously low; the ratio of the areas [curve (c)] fits the established pattern.} Figure 7 shows the actual valence emission (inelastically scattered electrons subtracted) at $h\nu = 18.0$ eV. The curves are corrected for the distortion introduced by the CMA which corresponds to a reduction of the emission by a factor E_p/E_k for kinetic energy E_k. (E_k in eV is numerically equal to the retarding voltage in volts.) E_p is the pass energy of the CMA. In Fig. 7 we observe the attenuation described by curve (d) of Fig. 6 as well as the increased valence emission. For the largest exposures, Fig. 7 roughly presents the VBDOS of the oxide of Bi.

From the EDC's it is evident that a band gap has opened up. The valence-band maximum has shifted down 1.9 eV below the Fermi level. With the help of the CFS's we can determine the minimum value for the band gap explicitly. First, a correct explanation of the structures appearing in the CFS's must be given.

The attractiveness of the CFS is that it is sensitive to the presence of electrons originating from the Auger decay of core hole states. The number

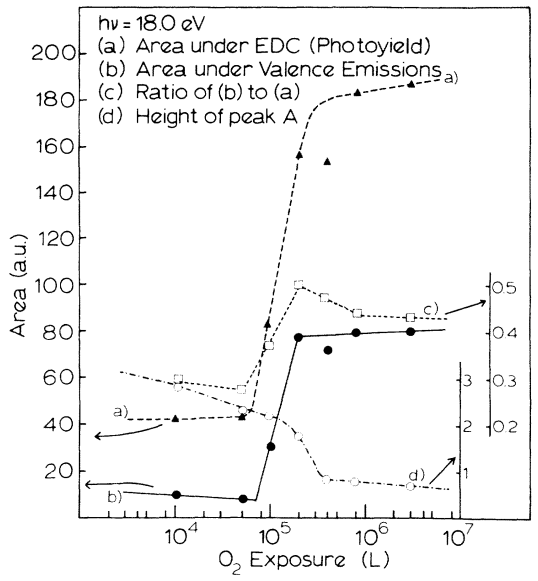

FIG. 6. Behavior of features of EDC's at $h\nu = 18.0$ eV as a function of O_2 exposure. The curve labeled (a) is the numerical area under the EDC's, corrected for the attenuation of the CMA, and is representative of the total photoyield. The curve labled (b) is the corresponding valence emissions of the same EDC's with the inelastic peak subtracted. Curve (c) is just the ratio of curve (b) to curve (a). Curve (d) is the corrected height of peak A in Fig. 3.

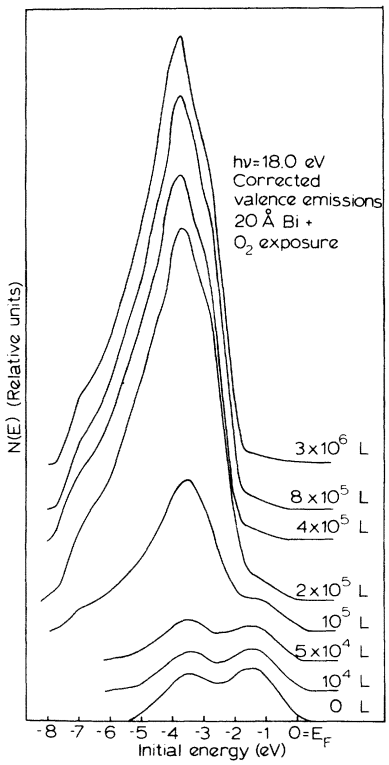

FIG. 7. Valence emissions from EDC's at $h\nu = 18.0$ eV (inelastic peak subtracted). This shows the growth of emissions associated with oxygen as well as attenuation of emissions associated primarily with Bi.

of such electrons at a given photon energy is proportional to the optical transition rate between the core state and the empty conduction state.[16] Thus, the CFS reproduces the optical joint density of states, or in this case, we could say it reproduces the CBDOS modulated by the matrix elements between the core state (single energy level) and the conduction band. In Bi this is especially useful because the $5d$ core states are spin-orbit split by 3.1 eV—enough so that the lower part of the conduction band is probed separately by two sets of nonoverlapping transitions. As will be seen, this also gives an opportunity for discussion of the angular momentum character of the conduction band.

In Fig. 5, for pure Bi, we see two large asymmetric peaks U and V. These have maxima at $h\nu = 24.5$ and 27.6 eV and are respectively due to the decay of the $5d_{5/2}$ and $5d_{3/2}$ core holes. The low-energy onset of each gives the location of the core level below the conduction-band minimum. The onsets are found at $h\nu = 23.8$ and 26.9 eV which are the locations of the $5d_{5/2}$ and $5d_{3/2}$ core states below the Fermi level in metallic Bi. Note that the peaks are similarly shaped, indicating that the two core states produce comparable matrix elements with the conduction band. That is, the joint densities of states between the two core levels and the conduction band are similar.

In Fig. 5 are shown several other CFS's which show the effect of ever increasing exposures to oxygen. For the most heavily oxidized situation, vastly different structures emerge, and peaks U and V have almost vanished. Structures appear at higher photon energies, and do not seem to have any similarities to the structures appearing for pure Bi. However, from the EDC's at $h\nu = 38.0$ eV, we know that the Bi $5d$ levels have shifted 1.9 eV deeper below the Fermi energy. It is interesting to note that the leading edges of peaks X and Z are found at $h\nu = 25.7$ and 28.8 eV. These edges are separated by 3.1 eV and are, respectively, just 1.9 eV higher in photon energy than the leading edges of peaks U and V in pure Bi. These considerations show that all structures between $h\nu = 25.7$ and 28.8 eV are due to the decay of the Bi $5d_{5/2}$ core hole in Bi_2O_3, whereas, all structures at higher photon energies are due primarily to decay of the Bi $5d_{3/2}$ core hole in Bi_2O_3. (We say Bi_2O_3 because it is the common oxide, although we may not have a stoichiometric composition.) The energetics of the Auger process support this conclusion. The maximum kinetic energy of an electron emitted during an Auger process and passing through the CMA is

$$E_{max} = E_{VBM} - E_{5d} - (\phi_A - E_{VBM}) , \quad (1)$$

where E_{VBM} is the energy of the valence-band maximum, E_{5d} is the energy of the core state, and ϕ_A is the work function of the CMA, with the Fermi level taken as the reference and the zero of energy as illustrated in Fig. 8. For the $5d_{5/2}$ state, Eq. (1) gives $E_{max} = 17.40 \pm 0.1$ eV; and for the $5d_{3/2}$ state, $E_{max} = 20.50 \pm 0.1$ eV. CFS's made at kinetic energies of 18.0 and 19.0 eV showed peak Z. This does not rule out contributions from the $5d_{5/2}$ state at lower kinetic energies, but would suggest that such contributions are much weaker than the predominant structure due to the $5d_{3/2}$ state in that photon energy range. Such being the case, the CBDOS may be divided into two main regions just above the minimum. The lower one-third is predominantly of $6p_{1/2}$ character, since transitions from the $5d_{5/2}$ state would be dipole forbidden altogether, but transitions from the $5d_{3/2}$ state would be permitted. The upper two-thirds of the region should consist mostly of $6p_{3/2}$-like states since the transitions from the $5d_{5/2}$ level appear to be stronger than those from the $5d_{3/2}$ state. The latter transitions show up as only a shoulder on the high-energy side of the peak Z. These results are summarized in Table I. A situation similar to this showed up in optical data on lead chalcogenides presented by Martinez *et al.*,[17] where the lower part of the conduction band was not coupled to the Pb $5d_{5/2}$ core state.

The valence and filled conduction bands of Bi as calculated by Golin[7] are extended in nature, i.e., they are not flat bands, although the density of states shows two peaks. The peaks are broad,

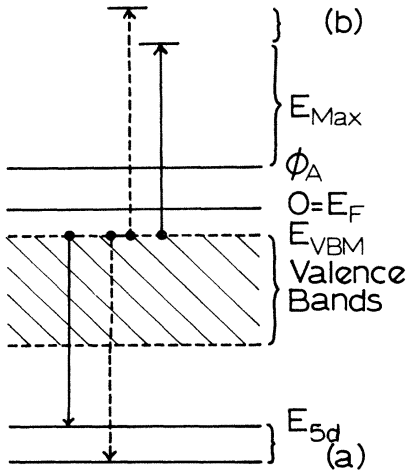

FIG. 8. Schematic diagram for determining maximum final energy of an Auger electron. The region (b) contains all final energies which may occur only for the decay of the deeper of the two core levels (a). The maximum final energy results when both the electron filling the core hole and the photoemitted electron originate at the top of the valence band.

TABLE I. Details about the conduction bands of Bi and its oxide. "Core decaying" refers to the cause of the detected Auger electrons, and "angular momentum character" denotes the interpretation of the evidence of the nature of the lower features of the empty conduction bands.

Peak	Photon energy (eV) Peak	Onset	Core decaying	Angular momentum character
U (Bi)	24.5	23.8	$5d_{5/2}$	$6p$, mixed
V (Bi)	26.7	26.9	$5d_{3/2}$	$6p$, mixed
X (oxide)	26.2	25.7	$5d_{5/2}$	small component of $6p_{3/2}$ [a]
Y (oxide)	27.3	···	$5d_{5/2}$	largely $6p_{3/2}$ [b]
Z (oxide)	29.25	28.8	$5d_{3/2}$	mostly $6p_{1/2}$ [a]
shoulder (oxide)	30.4	···	$5d_{3/2}$	largely $6p_{3/2}$ [b]

[a] The selection rules applied to transitions to these bands from the core states leads to the statement that the lower conduction band is $6p_{1/2}$-like.

[b] The transition strengths from a $5d_{3/2}$ state to a $6p_{1/2}$ or $6p_{3/2}$ are in the ratio 5:1 implying the upper region is really mostly $6p_{3/2}$-like.

corresponding to regions of $\vec{k}$ space where the bands are less extended—but not particularly flat. The empty conduction bands are quite extended and there is considerable mixing of $6p_{1/2}$ and $6p_{3/2}$ states in the bands. Our results show that in the oxide, the lower part of the conduction band is very flat—almost atomiclike. The width of peak Z in Fig. 5 is of the order of 0.5 eV and the above-mentioned dipole selection rule is atomic in origin. That the selection rule is broken is an indication of $\vec{k}$ dependence in the band, and that there is a small admixture of $6p_{3/2}$ states into the predominantly $6p_{1/2}$ band. It should not be forgotten that the $5d$ core states are very localized and the spatial extent of the region of overlap of the $5d$ states with the $6p$ states in Bi is expected to be small. The narrowness of peak Z (also peak X) indicates the degree of localization of the $6p$ orbitals on the Bi atoms; there is considerably less broadening of the $6p$ states than in pure Bi. As a final comment on the nature of the conduction band, we recall that the filled conduction bands in Bi are spin-orbit split, but have considerable overlap. In the oxide, the empty conduction bands are still spin-orbit split, but with little overlap. The peaks A and B in the EDC at $h\nu = 18.0$ eV for Bi show both the spin-orbit splitting and the overlap. The peaks X and Y or Z and Y in the CFS for the oxide show the spin-orbit splitting in the empty conduction bands. The presence of a shoulder in the CFS for the oxide at $h\nu \sim 30.4$ eV confirms the $6p_{3/2}$ nature of the upper part of the conduction band. The dipole transition $5d_{3/2} \rightarrow 6p_{3/2}$ is only about $\frac{1}{5}$ the strength of the transition $5d_{3/2} \rightarrow 6p_{1/2}$ (using strictly atomic functions).

The shift by 1.9 eV of the CFS structures is just the same as the downward movement by the core states. When Bi oxidizes, the $6p$ electrons just below the Fermi level become covalently bonded with the O $2p$ orbitals. This depletion is observed in Figs. 1–3 as well as Fig. 7. The growth of the peak at $E = -3.7$ eV corresponds to the addition of oxygen and coincides with the depletion of the electrons at the Fermi level. This is also seen in chemisorption studies, where a strong oxygen resonance appears at about the same energy (below the vacuum level) when O is present.[18–20] The yellowish color of Bi_2O_3 also suggests a band gap of the order of 2 eV. In fact, we can only state a minimum value for the band gap, since the exact location of the conduction band minimum may be shaded by core-excitonic effects. There seems to be no reliable optical data on Bi_2O_3 with which to resolve the issue.

Plots of the type shown in Fig. 6 could be made for each film studied, and the features would be much the same. What would differ is the critical exposure (and/or pressure) at which strong oxidation would begin, and perhaps the rate at which the process occurred. It may be argued that a critical pressure need be exceeded for the onset of strong oxidation, but the oxidation is not an instantaneous process—it continues with increasing exposure at the same pressure. There was one exception, however: a single monolayer film (~3 Å) showed strong adsorption of oxygen but there was no shift in the core states. The monolayer of Bi produced structures in the CFS's reminiscent of thicker films, but substrate features were still visible, even if attenuated.

Other factors entering into the nature of the film and its behavior were the quality of the substrate

and the thickness and means by which the film was laid down.[11] A film was made on a polished Cu substrate which was nominally orders of magnitude rougher than the cleaved crystals of the V*B*-VI*B* layered compounds which were used as substrates. A good cleave of one of them is atomically smooth and relatively inert.[10,21] For the film discussed here, the onset of strong oxidation occurred between 5×10^4 L and 10^5 L of O_2. (This film was made in several different evaporations.[11]) The film on Cu had an onset at a slightly lower exposure, and films made in a single evaporation in general did not show strong oxidation until exposures of the order of 10^6 L. In other words, the oxidation of the smoother films (presumably on fine substrates and grown continuously) was somewhat retarded in comparison to the rougher films. If quantitative oxidation kinetics are to be done on Bi, they should be done on clean crystalline surfaces.

Finally, we would like to compare our CFS data with electron-energy-loss spectra (ELS) for both Bi and oxidized Bi.[22] The ELS's for Bi show the Bi 5*d* states at photon energies comparable to those we found in our CFS's; i.e., the transitions from the 5*d* cores occur at the same energies. For Bi films oxidized by heating in humid air, the ELS shows a single peak at about $h\nu = 29$ eV, again comparable to the optical transitions observed in our CFS's. Interestingly, earlier ELS measurements of Bi films showed all three peaks[23] (i.e., peaks *U*, *V*, and *Z*), although the later work shows that the earlier data was probably taken on contaminated or partially oxidized films.[22] For the oxidized Bi films, no other nearby structures were noted.[22] This points out the relative sensitivity of CFS compared to ELS, at least when surface sensitivity need be considered. Further, it is to be noted that CFS may be done only with a continuum source such as provided by the electron storage ring. The techniques exploited in this paper, when combined with other surface-sensitive techniques (e.g., low-energy-electron diffraction and Auger electron spectroscopy) could lead to more complete and quantitative investigations of surfaces and surface processes.

V. SUMMARY

Three phases of ultraviolet photoemission have been used to make a study of the oxidation of thin Bi films. It was found that oxidation takes place by means of a precursor stage, a nucleation process, and then a stable oxide growth to a moderate thickness. These observations were made from the behavior of the electronic states of Bi and the oxidized Bi. Upon oxidation, a band gap of about 1.9 eV opens, and the binding energy of the 5*d* core levels increases by about the same amount. In the oxide, the bottom of the conduction band is found to have a definite $6p_{1/2}$-like angular momentum character, while the next upper portion is found to be $6p_{3/2}$-like, showing localization and spin-orbit splitting of the empty conduction states.

ACKNOWLEDGMENTS

We would like to express our gratitude to Ednor M. Rowe and the staff of the Synchrotron Radiation Center for their fine support during this entire project. Appreciation is also extended to R. A. Omar who assisted in taking the data.

---

*Work supported by NSF Contract No. DMR-74-02609A01.
†Work performed on the Electron Storage Ring of the University of Wisconsin Synchrotron Radiation Center, P. O. Box 6, Stoughton, Wisc. 53589. Operation of the Electron Storage Ring and the SRC is made possible by NSF Grant No. DMR-74-15089.

[1]P. E. Gregory, P. Chye, H. Sunami, and W. E. Spicer, J. Appl. Phys. 46, 3525 (1975).
[2]C. R. Helms and W. E. Spicer, Phys. Rev. Lett. 28, 565 (1972); Appl. Phys. Lett. 21, 237 (1972).
[3]I. Lindau and W. E. Spicer, J. Appl. Phys. 45, 3520 (1974).
[4]D. M. Collins, J. B. Lee, and W. E. Spicer, Phys. Rev. Lett. 35, 592 (1975).
[5]G. Brodén and T. N. Rhodin, Faraday Disc. Chem. Soc. 60, 112 (1975).
[6]L. Ley, R. A. Pollak, S. Kowalczyk, F. R. McFeely, and D. A. Shirley, Phys. Rev. B 8, 641 (1973).
[7]Luiz G. Ferreira, J. Phys. Chem. Solids 28, 1891 (1967); Stuart Golin, Phys. Rev. 166, 643 (1968).
[8]G. J. Lapeyre, A. D. Baer, J. Hermanson, J. Anderson, J. A. Knapp, and P. L. Gobby, Solid State Commun. 15, 1601 (1974); Z. Hurych, J. C. Shaffer, D. L. Davis, T. A. Knecht, G. J. Lapeyre, P. L. Gobby, J. A. Knapp, and C. G. Olson, Phys. Rev. Lett. 33, 830 (1974).
[9]Z. Hurych, D. Davis, D. Buczek, C. Wood, G. J. Lapeyre, and A. D. Baer, Phys. Rev. B 9, 4392 (1974).
[10]Z. Hurych and R. L. Benbow (unpublished).
[11]Some of the films were used for other studies and were evaporated in layers at different times. Some were grown on surfaces resulting from excellent cleaves while others were grown on surfaces resulting from mediocre cleaves. Varying thicknesses were used. All of these contributed to the differences noted in Sec. IV.
[12]G. J. Lapeyre, T. Huen, and F. Wooten, Solid State

Commun. 8, 1233 (1970).
[13]Unfortunately, we were unable to measure accurately the work function of Bi or its oxide, so we could not monitor changes in the work function. (The work function of the layered compounds is large—so they were mounted in direct contact with the system ground.) This turns out not to be a serious handicap to this study; we have sufficient information to comment on the oxidation of Bi.
[14]The work of Ref. 10 showed that a fraction of a monolayer of Bi is easily detected by CFS if it is on the surface because the Bi 5*d* core emissions are so prominent. On the other hand, some other metals such as Sr clearly maintain a metal-rich outer layer. See C. R. Helms and W. E. Spicer, Phys. Rev. Lett. 32, 228 (1974).
[15]See G. W. Simmons and D. J. Dwyer, Surf. Sci. 48, 373 (1975); A. J. Melmed and J. J. Carroll, J. Vac. Sci. Technol. 10, 164 (1973); P. B. Sewell, D. F. Mitchell, and M. Cohen, Surf. Sci. 33, 535 (1972); and references therein.
[16]W. Gudat and C. Kunz, Phys. Rev. Lett. 29, 169 (1972).
[17]G. Martinez, M. Schlüter, M. L. Cohen, R. Pinchaux, P. Thiry, D. Dagneaux and Y. Petroff, Solid State Commun. 17, 5 (1975).
[18]D. E. Eastman and J. K. Cashion, Phys. Rev. Lett. 27, 1520 (1971).
[19]J. M. Baker and D. E. Eastman, J. Vac. Sci. Technol. 10, 223 (1973).
[20]D. Menzel, J. Vac. Sci. Technol. 12, 313 (1975), and references therein.
[21]D. Haneman, Phys. Rev. 119, 567 (1960).
[22]C. Wehenkel and B. Gauthé, Solid State Commun. 15, 555 (1974).
[23]B. Gauthé and C. Wehenkel, Phys. Lett. A 39, 171 (1972), and references therein.